

ON THE GENERALIZATION OF SFT: A REINFORCEMENT LEARNING PERSPECTIVE WITH REWARD RECTIFICATION

Yongliang Wu^{1*} **Yizhou Zhou**^{2*†} **Zhou Ziheng**³ **Yingzhe Peng**¹ **Xinyu Ye**⁴
Xinting Hu⁵ **Wenbo Zhu**⁶ **Lu Qi**⁷ **Ming-Hsuan Yang**⁸ **Xu Yang**^{1‡}

¹Southeast University ²Independent Researcher ³University of California, Los Angeles

⁴Shanghai Jiao Tong University ⁵Nanyang Technological University

⁶University of California, Berkeley ⁷Wuhan University ⁸University of California, Merced

yongliang0223@gmail.com, zyz0205@hotmail.com, xuyang_palm@seu.edu.cn

ABSTRACT

In this work, we present a simple yet theoretically motivated improvement to Supervised Fine-Tuning (SFT) for the Large Language Model (LLM), addressing its limited generalization compared to reinforcement learning (RL). Through mathematical analysis, we reveal that standard SFT gradients implicitly encode a problematic reward structure that may severely restrict the generalization capabilities of model. To rectify this, we propose Dynamic Fine-Tuning (DFT), stabilizing gradient updates for each token by dynamically rescaling the objective function with the probability of this token. With just a single-line change, the method outperforms standard SFT on multiple difficult benchmarks and base models, from math reasoning to code generation and multi-modal tasks, demonstrating improved generalization. Additionally, DFT achieves competitive results in offline RL settings, providing an effective yet streamlined alternative. By bridging theoretical insights with practical solutions, this work advances the state of SFT. The code will be available at <https://github.com/yongliang-wu/DFT>.

1 INTRODUCTION

Supervised Fine-Tuning (SFT), which adapts models to expert demonstrations, has become the standard post-training paradigm for Large Language Models (LLMs). It enables efficient task adaptation and capability enhancement (Chung et al., 2024; Zhang et al., 2024b; Sanh et al., 2022; Ouyang et al., 2022), and is popular for its ease of implementation and rapid acquisition of expert-like behaviors (Wei et al., 2022; Zhou et al., 2023). Despite these advantages, SFT often shows limited generalization compared to reinforcement learning (RL) (Chu et al., 2024; Ouyang et al., 2022; Christiano et al., 2017; Bai et al., 2022; Huan et al., 2025; Swamy et al., 2025). RL leverages explicit reward or verification signals to explore diverse strategies and thus generalizes better. However, RL requires substantial computation, careful hyperparameter tuning, and explicit reward signals—conditions often impractical in real-world settings (Schulman et al., 2017; Ouyang et al., 2022; Sheng et al., 2025; Strubell et al., 2019; Liu & Yin, 2024; Winsta, 2025). Moreover, RL can struggle to recover expert-like behaviors that SFT captures efficiently (Mandlekar et al., 2022; Chen et al., 2025b).

To exploit the complementary strengths of both approaches, many hybrid methods combine SFT with RL (Ouyang et al., 2022; Sheng et al., 2025; Rafailov et al., 2023; Liu et al., 2025; Qiu et al., 2025). Yet a key question remains: can SFT itself be fundamentally improved? This is crucial, as SFT remains the only viable option when datasets contain only positive demonstrations, with no negative samples or reward model available.

In this work, we address this gap with a mathematical analysis of the connection between SFT and RL. We show that SFT’s gradient update is equivalent to a policy gradient with a specific, implicitly defined reward. Crucially, this reward is (i) sparse, and (ii) inversely proportional to the model’s

*Equal Contribution. †Project Leader. ‡Corresponding Author.

probability of expert actions (see equation 6). As a result, when the model assigns low probability to expert actions, the gradient becomes excessively large—yielding an ill-posed reward structure and unstable, overfitting-prone optimization.

Building on this insight, we propose Dynamic Fine-Tuning (DFT), a principled fix. Our method rescales the SFT objective at each token by its probability, canceling the distortion introduced by inverse-probability weighting. This transforms the SFT gradient from an unstable, biased estimator into a stable, uniformly weighted update rule.

Empirically, DFT delivers substantial improvements. On the Qwen-2.5-Math series (Qwen Team et al., 2024b) fine-tuned with NuminaMath-CoT (Li et al., 2024), DFT yields gains several times larger than standard SFT. More importantly, unlike SFT, which often degrades on challenging benchmarks such as OlympiadBench (He et al., 2024), AIME 2024 (American Institute of Mathematics, 2024), and AMC 2023 (Mathematical Association of America, 2023), our method consistently improves performance and generalization. These improvements hold across models, scales, and data sizes (Table 1, Figure 1), and extend to code generation and multimodal reasoning (Tables 3, 4).

We further test DFT in off-policy RL settings (Table 2), where dense rewards are available (Levine et al., 2020). Our method not only outperforms offline RL approaches such as DPO (Rafailov et al., 2023) and RAFT (Dong et al., 2023; Ahn et al., 2024), but also achieves competitive or superior performance to online methods like GRPO and PPO on math tasks with Qwen2.5-Math-1.5B. Unlike these RL methods, DFT requires neither a reference model nor large batch sizes, making it a simpler and more resource-efficient alternative.

To understand its effect, we analyze token probability distributions after training (Figure 2). While traditional SFT uniformly pushes probabilities toward the training set, DFT selectively increases some while reducing others. In particular, the proportion of less strongly fitted tokens rises, suggesting improved regularization and reduced overfitting. We provide further discussion in Appendix A.4.

The contributions of this work are theoretical and practical. On the theoretical side, we mathematically establish LLM SFT as a special RL in policy gradient space, pinpoint the underlying reasons for the limited generalization of SFT, and derive a method to improve it. On the experimental side, we show that such a simple solution, just one line of code, can enhance the performance and generalization capabilities of SFT across various tasks and models.

2 RELATED WORK

The trade-off between supervised fine-tuning (SFT) and reinforcement learning (RL) is central to the alignment of large language models. SFT is widely adopted due to its simplicity and efficiency in imitating expert demonstrations (Chung et al., 2024; Zhou et al., 2023; Wei et al., 2022), analogous to behavioral cloning in robotics (Sammut, 2011; Mandlekar et al., 2022). However, the literature consistently highlights its limitations, particularly the tendency to overfit and generalize poorly compared to RL, which leverages reward signals to discover more robust policies (Ouyang et al., 2022; Christiano et al., 2017; Bai et al., 2022; Swamy et al., 2025; Zhang et al., 2025). A recent systematic comparison by Chu et al. (2024) across textual and visual domains confirms this distinction, concisely summarized as “SFT memorizes while RL generalizes.” They further show that SFT remains indispensable as an initialization step, stabilizing output formatting prior to effective RL training. Nonetheless, RL faces significant practical hurdles, including computational expense, sensitivity to hyperparameters, and the requirement of an explicit reward function, all of which constrain its applicability (Schulman et al., 2017; Strubell et al., 2019; Sheng et al., 2025).

To combine the strengths of both paradigms, much recent work has pursued hybrid approaches. The most common strategy involves SFT pretraining followed by RL-based refinement with a learned reward model, as popularized by InstructGPT (Ouyang et al., 2022). More recent methods interleave SFT and RL updates to improve stability and performance (Sheng et al., 2025; Liu et al., 2025; Qiu et al., 2025). Other approaches, such as Direct Preference Optimization (DPO) (Rafailov et al., 2023), bypass reward modeling entirely by directly optimizing policies on preference data, thereby unifying imitation and reinforcement signals within a single loss function. Chen et al. (2025a) introduce Negative-aware Fine-Tuning (NFT), which models incorrect generations via an implicit negative policy, enabling self-improvement without explicit feedback. While powerful, these methods rely on reward signals, preference pairs, or negative samples. They enrich the training pipeline

but do not fundamentally improve SFT in its native setting, where only positive demonstrations are available. Our work instead focuses on enhancing SFT itself without requiring external feedback.

A complementary line of theoretical research seeks to unify SFT and RL under a common formalism. Du et al. (2025) reinterpret RLHF as a reward-weighted variant of SFT, preserving reliance on an explicit reward. Wang et al. (2025) show that SFT can be cast as RL with an implicit reward, proposing adjustments such as smaller learning rates to manage the vanishing KL constraint. Abdolmaleki et al. (2025) analyze learning from both positive and negative feedback, studying how their balance affects convergence. Qin & Springenberg (2025) view SFT as a lower bound of RL and introduce importance weighting based on the data-generating policy. While these works establish connections between SFT and RL through weighting, they do not provide a precise mathematical equivalence between the SFT gradient and the offline policy gradient. Some methods approximate this connection in practice by reweighting training losses. For instance, MixCE (Zhang et al., 2023) combines the forward and reverse KL divergences to form a unified objective, while GOLD (Pang & He, 2021) adopts offline RL with demonstrations, introducing reliance on an unknown demonstration distribution π_b and a restrictive $1/N$ assumption. In contrast, our work rigorously establishes this equivalence, pinpointing the inverse-probability weighting term in SFT as the key distinction. This observation directly motivates our proposed solution: multiplying the SFT loss by the model probability to eliminate the weighting.

Interestingly, our method modifies the standard cross-entropy (CE) loss in a way that inverts the weighting philosophy of the widely used Focal Loss (Lin et al., 2017). Specifically, our modified CE takes the form $-p \log(p)$, whereas focal loss is defined as $-(1-p)^\gamma \log(p)$. Focal Loss deliberately downweights well-classified samples to emphasize underrepresented or hard cases, whereas we deliberately downweight poorly classified samples to encourage generalization. This inversion reflects a fundamental shift in the LLM era: while underfitting was once a central challenge, overfitting and memorization now dominate, demanding a rethinking of objective design.

3 METHOD

3.1 PRELIMINARIES

Supervised Fine-Tuning. Let $\mathcal{D} = \{(x, y^*)\}$ denote a corpus of expert demonstrations, where y^* is the complete reference response to the query x . SFT minimizes the sentence-level cross-entropy:

$$\mathcal{L}_{\text{SFT}}(\theta) = \mathbb{E}_{(x, y^*) \sim \mathcal{D}} [-\log \pi_\theta(y^* | x)]. \quad (1)$$

Its gradient is:

$$\nabla_\theta \mathcal{L}_{\text{SFT}}(\theta) = \mathbb{E}_{(x, y^*) \sim \mathcal{D}} [-\nabla_\theta \log \pi_\theta(y^* | x)]. \quad (2)$$

Reinforcement Learning. Let y denote a response sampled from the policy $\pi_\theta(\cdot | x)$ for query x . Given a reward function $r(x, y) \in \mathbb{R}$, the policy objective is

$$J(\theta) = \mathbb{E}_{x \sim \mathcal{D}_x, y \sim \pi_\theta(\cdot | x)} [r(x, y)]. \quad (3)$$

Its policy gradient at the sentence level is

$$\nabla_\theta J(\theta) = \mathbb{E}_{x \sim \mathcal{D}_x, y \sim \pi_\theta(\cdot | x)} [\nabla_\theta \log \pi_\theta(y | x) r(x, y)]. \quad (4)$$

3.2 UNIFY SFT AND RL GRADIENT EXPRESSION

Rewriting SFT Gradient as Policy Gradient via Importance Sampling. The SFT gradient in equation 2 is taken under the *fixed* demonstration distribution. We convert it to an on-policy expectation by inserting an importance weight that compares the expert (Dirac Delta) distribution with the model distribution.

$$\mathbb{E}_{(x, y^*) \sim \mathcal{D}} [-\nabla_\theta \log \pi_\theta(y^* | x)] = \mathbb{E}_{x \sim \mathcal{D}_x} \underbrace{\mathbb{E}_{y \sim \pi_\theta(\cdot | x)} \frac{\mathbf{1}[y = y^*]}{\pi_\theta(y | x)} [-\nabla_\theta \log \pi_\theta(y | x)]}_{\text{resample + reweight}} \quad (5)$$

Define the auxiliary variables (importance sampling weight) as

$$w(y | x) = \frac{1}{\pi_\theta(y | x)}, \quad r(x, y) = \mathbf{1}[y = y^*].$$

Reorganizing equation 5 and rewriting it using the above auxiliary variables, we obtain the form

$$\nabla_{\theta} \mathcal{L}_{\text{SFT}}(\theta) = -\mathbb{E}_{x \sim \mathcal{D}_x, y \sim \pi_{\theta}(\cdot | x)} [w(y | x) \nabla_{\theta} \log \pi_{\theta}(y | x) r(x, y)]. \quad (6)$$

This form of the SFT gradient now aligns closely with the policy gradient equation 4. Thus we can see, *conventional SFT is precisely an on-policy-gradient with the reward as an indicator function of matching the expert trajectory but biased by an importance weighting $1/\pi_{\theta}$* . More detailed derivations can be found in Appendix A.3.

Given the unavoidable sparsity of reward signals in the SFT setting, we identify the importance sampling weight $1/\pi_{\theta}$ as a fundamental cause of the poor generalization of SFT relative to RL. When the model assigns low probability to the expert response, the weight w becomes excessively large, leading to an ill-posed reward structure. In such cases, the gradient can grow disproportionately, making the training unstable and prone to overfitting. This issue is further exacerbated by the extreme sparsity of the reward function, since $r(x, y) = 1[y = y^*]$ is non-zero only when the model exactly matches the expert output. As a result, optimization tends to overfit rare exact-match demonstrations, undermining the model’s ability to generalize beyond training data.

3.3 PROPOSED METHOD

Reward Rectification via Dynamic Reweighting. To neutralize the skewed reward issue identified when viewing SFT under the RL objective, we dynamically reweight the reward by multiplying by a corrective inverse ratio given by the policy probability $1/w$. The resulting “dynamically fine-tuned” gradient is then

$$\nabla_{\theta} \mathcal{L}_{\text{DFT}}(\theta) = \nabla_{\theta} \mathcal{L}_{\text{SFT}}(\theta) \cdot \text{sg}\left(\frac{1}{w}\right) = \nabla_{\theta} \mathcal{L}_{\text{SFT}}(\theta) \cdot \text{sg}(\pi_{\theta}(y^* | x)). \quad (7)$$

where $\text{sg}(\cdot)$ denotes the stop gradient operator, ensuring that gradients do not flow through the reward scaling term w . To facilitate transition to later equations, we directly write $1/w$ to be $\pi_{\theta}(y^* | x)$ instead of $\pi_{\theta}(y | x)$ because the indicator function in equation 5 or equation 6 would leave all cases where $y \neq y^*$ is 0. Now since the gradient does not flow, the corrected SFT loss also becomes a simple reweighted loss, called Dynamic Fine-tuning (DFT).

$$\mathcal{L}_{\text{DFT}}(\theta) = \mathbb{E}_{(x, y^*) \sim \mathcal{D}} [\text{sg}(\pi_{\theta}(y^* | x)) \log \pi_{\theta}(y^* | x)]. \quad (8)$$

However, in practice, computing importance weights over the entire trajectory can induce numerical instability. A common treatment of this issue is to simply apply importance sampling at the token level, as was adopted in PPO (Schulman et al., 2017). This leads to the final DFT loss version:

$$\mathcal{L}_{\text{DFT}}(\theta) = \mathbb{E}_{(x, y^*) \sim \mathcal{D}} \left[-\sum_{t=1}^{|y^*|} \text{sg}(\pi_{\theta}(y_t^* | y_{<t}^*, x)) \log \pi_{\theta}(y_t^* | y_{<t}^*, x) \right]. \quad (9)$$

Note that the reward of this corrected SFT (in RL form), i.e., DFT, now becomes 1 uniformly for all expert trajectory. This is akin to contemporary verification based reward approach RLVR (DeepSeek-AI et al., 2025) that assigns uniform reward to all correct samples. Consequently, it avoids over-concentration on specific low-probability reference tokens, leading to more stable updates and improved generalization without introducing any additional sampling or reward models.

4 EXPERIMENTS

We design four groups of experiments to comprehensively evaluate DFT. We first study the standard SFT setting on mathematical reasoning tasks to establish its core advantage over SFT (Section 4.1). We then extend to an offline RL setting, comparing DFT with representative offline and online RL methods (Section 4.2). To test cross-domain robustness, we further examine DFT on code generation benchmarks (Section 4.3) and its applicability to multi-modal reasoning math datasets (Section 4.4).

Table 1: Average@16 accuracy of five state-of-the-art large language models on mathematical reasoning benchmarks. The best performance of each model across benchmarks is bold.

	Math500	Minerva Math	Olympiad Bench	AIME24	AMC23	Avg.
LLaMA-3.2-3B	1.63	1.36	1.01	0.41	1.56	1.19
LLaMA-3.2-3B w/SFT	8.65	2.38	2.06	0.00	3.13	3.24
LLaMA-3.2-3B w/DFT	12.79	2.84	2.90	0.83	3.91	4.65
LLaMA-3.1-8B	1.86	0.98	0.94	0.21	1.01	1.00
LLaMA-3.1-8B w/SFT	16.85	5.78	3.88	0.00	5.16	6.33
LLaMA-3.1-8B w/DFT	27.44	8.26	6.94	0.41	12.03	11.02
DeepSeekMath-7B	6.15	2.15	1.74	0.21	2.97	2.64
DeepSeekMath-7B w/SFT	26.83	7.26	6.33	0.41	8.28	9.82
DeepSeekMath-7B w/DFT	41.46	16.79	15.00	1.24	16.25	18.15
Qwen2.5-Math-1.5B	31.66	8.51	15.88	4.16	19.38	15.92
Qwen2.5-Math-1.5B w/SFT	43.76	13.04	12.63	1.87	18.75	18.01
Qwen2.5-Math-1.5B w/DFT	64.89	20.94	27.08	6.87	38.13	31.58
Qwen2.5-Math-7B	40.12	14.39	17.12	6.68	27.96	21.25
Qwen2.5-Math-7B w/SFT	53.96	16.66	18.93	2.48	26.09	23.62
Qwen2.5-Math-7B w/DFT	68.20	30.16	33.83	8.56	45.00	37.15

4.1 MAIN EXPERIMENT - MATHEMATICAL REASONING TASK

To examine whether DFT can outperform vanilla SFT across tasks, architectures, and scales, we use mathematical reasoning as a representative testbed.

4.1.1 SETUP AND IMPLEMENTATION DETAILS

To efficiently manage computational resources, We andomly sample 100,000 instances from the the NuminaMath-CoT dataset (LI et al., 2024) for training. We conduct experiments using multiple models, including Qwen2.5-Math-1.5B, Qwen2.5-Math-7B (Qwen Team et al., 2024a), LLaMA-3.2-3B, LLaMA-3.1-8B (Dubey et al., 2024), and DeepSeekMath-7B (Shao et al., 2024).

Our implementation builds upon the verl framework (Sheng et al., 2025), using recommended SFT hyper-parameters. Specifically, we employ the AdamW optimizer with learning rates of 5×10^{-5} for all models except the LLaMA-3.1-8B-Base, for which we adopt a lower learning rate of 2×10^{-5} . We set the mini-batch size to 256 and the maximum input length to 2048 tokens. The learning rate follows a cosine decay schedule with a warm-up ratio of 0.1. We evaluate on benchmarks including Math500 (Hendrycks et al., 2021), Minerva Math (Lewkowycz et al., 2022), Olympiad Bench (He et al., 2024), AIME 2024 (American Institute of Mathematics, 2024), and AMC 2023 (Mathematical Association of America, 2023) through the official Qwen2.5-Math evaluation pipeline (Qwen Team et al., 2024a). Each model uses the default chat template and Chain-of-Thought (CoT) prompting to stimulate step-by-step reasoning. All reported results represent average accuracy across 16 decoding runs, evaluated with a temperature of 1.0 and maximum generation length of 4096 tokens.

4.1.2 MAIN RESULTS

DFT consistently yields average performance improvements over base models compared to standard SFT across all benchmarks. Table 1 shows that, for Qwen2.5-Math-1.5B, DFT achieves an average gain of +15.66 points over the base model, which is over $5.9 \times$ larger than the +2.09 point improvement from SFT. This pattern generalizes across other model families and sizes: LLaMA-3.2-3B benefits from a +3.46 point gain with DFT, exceeding the SFT gain (+2.05) by approximately $1.4 \times$; LLaMA-3.1-8B achieves +10.02 from DFT, surpassing SFT's +5.33 by $1.88 \times$; DeepSeekMath-7B sees a +15.51 point improvement via DFT, which is $1.58 \times$ larger than SFT's +7.18; and Qwen2.5-Math-7B reaches a +15.90 point gain, nearly $3.8 \times$ higher than the SFT improvement of +2.37.

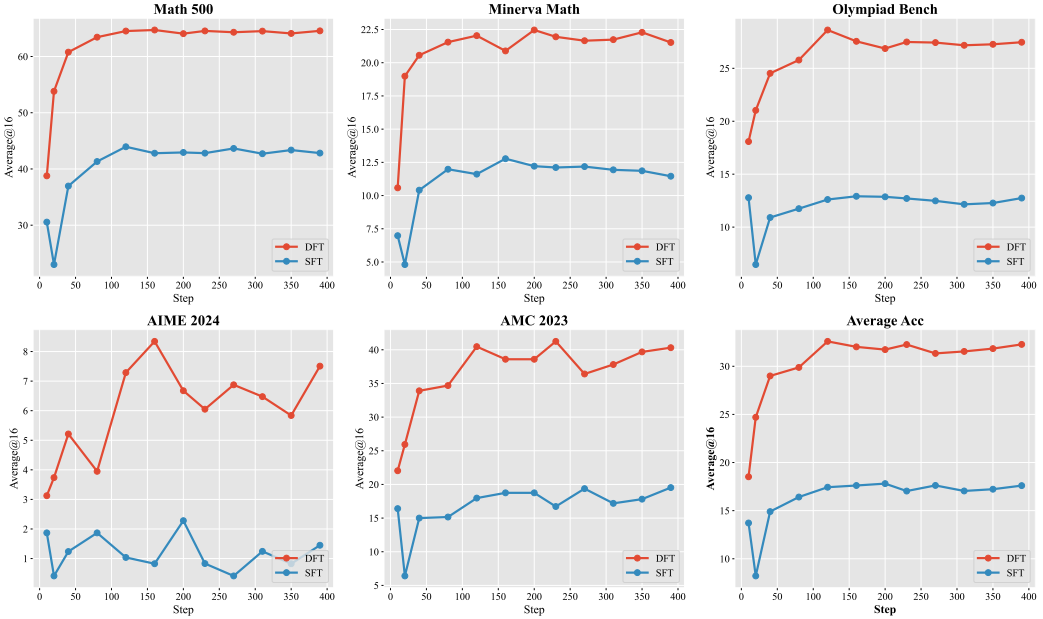


Figure 1: Accuracy progression for Qwen2.5-Math-1.5B across mathematical benchmarks, illustrating faster convergence and better performance achieved by DFT relative to SFT.

DFT demonstrates generalization and robustness, especially on challenging benchmarks where standard SFT yields minimal or even negative impact. For instance, on Olympiad Bench, SFT degrades performance for Qwen2.5-Math-1.5B, dropping accuracy from 15.88 to 12.63, while DFT boosts it to 27.08, +11.20 point improvement over base model. On AIME24, SFT reduces accuracy for Qwen2.5-Math-7B by 4.20 points (from 6.68 to 2.48), whereas DFT improves performance to 8.56, achieving a +1.88 point gain over the base model despite the difficulty of the benchmark. A similar trend is observed on AMC23. SFT reduces the performance of Qwen2.5-Math-1.5B from 19.38 to 18.75, while DFT raises it to 38.13, a +18.75 point gain over base. For Qwen2.5-Math-7B, SFT yields only a marginal improvement (+1.86), whereas DFT achieves a +17.04 point gain. These results underscore that DFT not only scales more effectively across models of varying capacities, but also exhibits better resilience on difficult reasoning tasks where traditional SFT struggles.

DFT exhibits better learning efficiency and faster convergence characteristics. Figure 1 reveals clear differences in learning dynamics between DFT and standard SFT on Qwen2.5-Math-1.5B across all math reasoning benchmarks. Compared to SFT, our method demonstrates three distinct advantages: (1) Faster convergence, achieving peak performance within the first 120 training steps on most benchmarks; (2) Better early-stage performance, with DFT already outperforming best final accuracy of SFT within the first 10–20 steps; and (3) Higher sample efficiency, consistently requiring fewer updates to reach relatively optimal results. This accelerated convergence shows that the dynamic reweighting mechanism in DFT leads to more informative gradient updates, guiding the model toward high-quality solutions early in training. It also suggests that DFT helps avoid the optimization plateaus or noise-prone regions often encountered in standard SFT, thereby enabling more efficient acquisition of complex mathematical reasoning patterns.

We also report the results of parameter-efficient fine-tuning (PEFT) training setting (Hu et al., 2022) and training on the OpenR1-Math dataset (Hugging Face, 2025) with better quality in Appendix A.7 and Appendix A.6, respectively. Comparison and Discussion with the concurrent method iw-SFT (Qin & Springenberg, 2025) is provided in Appendix A.5.

4.2 EXPLORATORY EXPERIMENT - OFFLINE RL SETTING

Equation 7 shows that SFT suffers from reward sparsity, since in a constructed dataset each query x has only a single reference answer y^* . From the perspective of RL, RFT/RAFT (Dong et al., 2023; Ahn et al., 2024) can be viewed as alleviating the sparse reward issue by effectively increasing

Table 2: Evaluation results on mathematical reasoning benchmarks in an offline reinforcement learning setting using reward signals from rejection sampling. The best performance is in bold.

	Setting	Math500	Minerva Math	Olympiad Bench	AIME24	AMC23	Avg.
Qwen2.5-Math-1.5B	–	31.66	8.51	15.88	4.16	19.38	15.92
Qwen2.5-Math-1.5B w/DPO	Offline	46.89	11.53	22.86	4.58	30.16	23.20
Qwen2.5-Math-1.5B w/RFT	Offline	48.23	14.19	22.29	4.37	30.78	23.97
Qwen2.5-Math-1.5B w/PPO	Online	56.10	15.41	26.33	7.50	37.97	28.66
Qwen2.5-Math-1.5B w/GRPO	Online	62.86	18.93	28.62	8.34	41.25	32.00
Qwen2.5-Math-1.5B w/DFT	Offline	64.71	25.16	30.93	7.93	48.44	35.43

reward density, thereby enhancing model performance. Motivated by this observation, we conduct an exploratory study applying DFT in an offline RL setting, where the reward sparsity problem is inherently less severe compared to standard SFT, to further validate the effectiveness.

4.2.1 SETUP AND IMPLEMENTATION DETAILS

We sample responses for 100,000 math questions using a temperature of 1.0 and generate four responses per question from the base model itself. Correct responses are identified using math verify and retained as training data, resulting in approximately 140,000 examples. For DPO training, we construct 100,000 positive–negative preference pairs from the generated responses.

We compare DFT with representative offline RL methods, including DPO (Rafailov et al., 2023) and RFT (Dong et al., 2023; Ahn et al., 2024), as well as online RL methods PPO (Schulman et al., 2017) and GRPO (Shao et al., 2024). For RFT and DFT, the training setup follows the configuration in Section 4.1. For DPO, we use the ms-swift (Zhao et al., 2024) with a learning rate of 1×10^{-6} , batch size of 128, and a warmup ratio of 0.05. For PPO and GRPO, training is performed using the verl (Sheng et al., 2025) with a learning rate of 1×10^{-6} , batch size of 256, and a warmup ratio of 0.1. We set the number of response $n = 4$ for GRPO.

4.2.2 RESULTS

DFT demonstrates competitive performance in the offline RL setting, outperforming both offline and online RL baselines. Table 2 shows DFT achieves an average score of 35.43, exceeding the best offline method RFT by +11.46 points, and even outperforming the strongest online RL algorithm GRPO by +3.43 points. Specially, on Math500, DFT scores 64.71, slightly ahead of GRPO (62.86) and better than PPO (56.10) and RFT (48.23). The gains are also notable on more challenging benchmarks: on AMC23, DFT achieves 48.44, a +7.19 point margin over GRPO and a +17.66 point gain over RFT. Similarly, on Minerva Math, DFT reaches 25.16, outperforming GRPO by +6.23 points, PPO by +9.75, and all offline baseline methods.

These results highlight the strength of DFT as a simple yet effective fine-tuning strategy. Despite its lack of iterative reward modeling or environment interaction, it provides a stronger learning signal than both offline methods like DPO/RFT and online policy optimization algorithms like PPO/GRPO in certain scale train set. This suggests that DFT can serve as a more efficient and scalable alternative to traditional RL pipelines, particularly in domains where preference supervision is available but reward modeling or online response sampling is expensive or impractical.

4.3 EXPLORATORY EXPERIMENT - CODE GENERATION TASK

To further validate the effectiveness of DFT, we investigate its performance on another reasoning-intensive task: code generation.

4.3.1 SETUP AND IMPLEMENTATION DETAILS

We adopt UltraFeedback (Cui et al., 2024) as the training dataset. From this corpus, we sample 10,000 prompts and, for each prompt, select the response with the highest average score to perform supervised fine-tuning (SFT) (Du et al., 2025). Model performance is assessed on three widely used code generation benchmarks: HumanEval (Chen et al., 2021), HumanEval+ (Liu et al., 2023),

Table 3: Performance of various models on code generation benchmarks. The best performance for each benchmark is highlighted in bold.

	HumanEval					MultiPL-E					
	HumanEval	HumanEval+	Python	C++	Java	PHP	TS	C#	Bash	JS	Avg.
Qwen2.5-3B	43.3	36.0	43.29	40.99	37.34	37.89	47.17	43.04	24.68	45.96	40.05
Qwen2.5-3B w/SFT	41.5	34.8	42.07	42.24	37.97	37.27	43.40	41.77	20.25	47.83	39.10
Qwen2.5-3B w/DFT	45.7	39.0	45.73	44.72	41.77	45.34	42.14	43.04	27.85	44.10	41.84
Qwen2.5-Coder-3B	52.4	42.7	51.83	53.42	46.20	47.20	54.09	55.06	25.32	54.04	48.39
Qwen2.5-Coder-3B w/SFT	51.8	43.9	51.22	51.55	48.10	54.66	59.12	51.27	34.18	54.04	50.52
Qwen2.5-Coder-3B w/DFT	56.7	50.0	57.32	54.66	51.27	58.39	58.49	60.76	31.01	53.42	53.16
Qwen2.5-Coder-7B	62.2	53.0	63.41	63.98	53.16	59.01	62.89	59.49	39.24	60.87	57.76
Qwen2.5-Coder-7B w/SFT	54.9	48.8	54.88	64.60	51.27	62.11	68.55	60.76	33.54	65.22	57.62
Qwen2.5-Coder-7B w/DFT	67.7	59.8	67.68	67.70	54.43	60.87	70.44	65.19	48.73	63.35	62.30

Table 4: Performance comparison across different multi-modal reasoning benchmarks. The best performance on each benchmark is highlighted in bold.

	MathVerse				MathVision	WeMath
	Vision Only	Vision Intensive	Vision Dominant	Overall		
Qwen2.5-VL-3B	28.81	30.96	31.60	33.83	21.25	4.10
Qwen2.5-VL-3B w/SFT	30.96	33.63	32.74	35.66	21.02	23.33
Qwen2.5-VL-3B w/DFT	32.49	35.91	33.50	37.54	22.30	23.71

and MultiPL-E (Cassano et al., 2023). Training is conducted for one epoch with a learning rate of 5×10^{-5} , a warm-up ratio of 0.05, and a batch size of 16.

4.3.2 RESULTS

Table 3 shows DFT achieves improvements in most cases compared to both base models and SFT. For Qwen2.5-3B, DFT raises HumanEval from 43.3 to 45.7 and HumanEval+ from 36.0 to 39.0, with the MultiPL-E average also increasing from 40.05 (base) and 39.10 (SFT) to 41.84. Similar trends are observed for Qwen2.5-Coder-3B, where DFT improves HumanEval to 56.7 and HumanEval+ to 50.0, outperforming both base and SFT. For Qwen2.5-Coder-7B, DFT reaches 67.7 on HumanEval, 59.8 on HumanEval+, and 62.3 average on MultiPL-E, surpassing SFT by +12.8, +11.0, and +4.7 points respectively. The overall trend demonstrates that DFT generally provides stronger performance across different models and languages.

4.4 EXPLORATORY EXPERIMENT - MULTI-MODAL REASONING

To further investigate the generalization of DFT, we extend our evaluation to multi-modal reasoning tasks that require both visual understanding and mathematical problem solving.

4.4.1 SETUP AND IMPLEMENTATION DETAILS

We use the WeThink dataset (Yang et al., 2025) for training. The model is fine-tuned using LLaMA-Factory (Zheng et al., 2024) and evaluated with VLMEvalKit (Duan et al., 2024). We train the model for 1 epoch with a learning rate of 5e-5. To comprehensively assess reasoning capabilities, we adopt a suite of multi-modal reasoning benchmarks including MathVerse (Zhang et al., 2024a), MathVision (Wang et al., 2024), and WeMath (Qiao et al., 2024) for evaluation.

4.4.2 RESULTS

DFT achieves consistent improvements over base models and SFT across all multi-modal reasoning benchmarks. Table 4 shows, on MathVerse, DFT boosts Qwen2.5-VL-3B from 33.83 to 37.54 average accuracy, outperforming the SFT gain of only +1.83 by +3.71 points. Consistent improvements are observed across all major vision-related subcategories. On MathVision, DFT improves performance from 21.25 (base) to 22.30, exceeding SFT which fails to provide gains (21.02). On

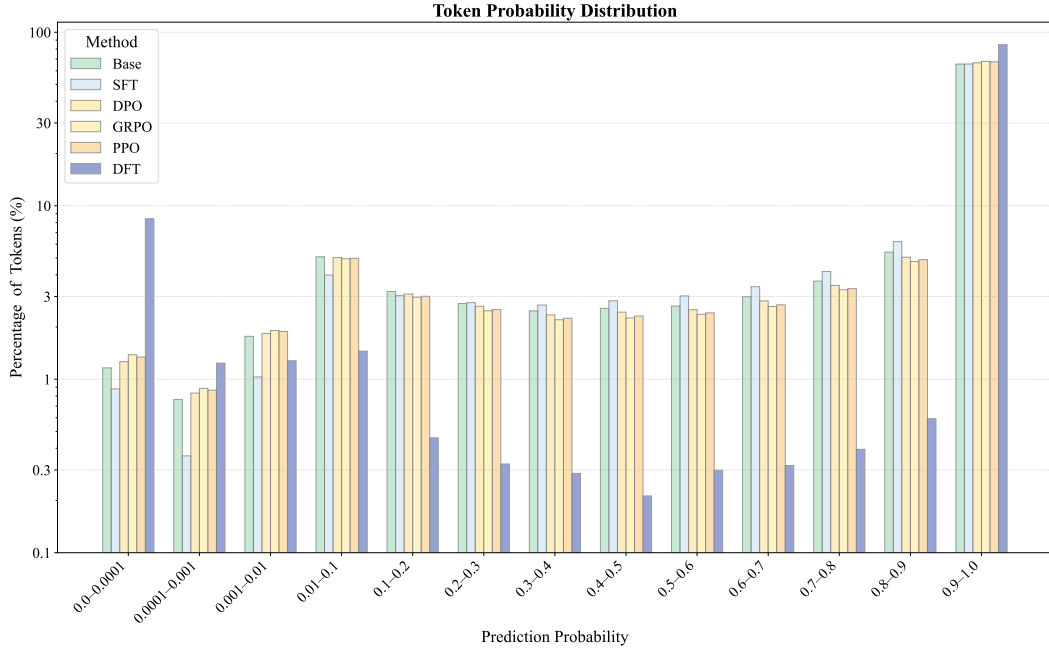


Figure 2: Token probability distributions on the training set before training and after fine-tuning with DFT, SFT, and various RL methods. A logarithmic scale is used on the y-axis for clarity.

WeMath, SFT already yields a +19.23 point gain, but DFT pushes performance slightly further to 23.71, maintaining superiority over both base and SFT. These results indicate that DFT not only strengthens text-only reasoning but also extends effectively to multi-modal domains.

4.5 ANALYSIS

To understand how the model trained by DFT is different from SFT and other RL methods, we look into the token probability distribution of the model’s output over the training set in Figure 2. SFT tends to uniformly increase token probabilities, shifting the entire distribution towards higher confidence, but mainly targeting the lower and lowest probability tokens. The highest probability token portion barely increases. In stark contrast, DFT exhibits a polarizing effect: it significantly boosts the probabilities of a subset of tokens while actively suppressing the probabilities of others. This leads to a bimodal distribution, with more tokens occupying both the highest and lowest probability bins. Other RL methods such as DPO, GPPO and PPO show the same trend as DFT, although the scale is much milder than it. We look into the words that belong to the lowest probability bin, and find that they are generally the conjunctive words or punctuations such as ‘the’, ‘let’, ‘;’, ‘.’ etc. These results suggest that for robust learning, models should not attempt to fit all tokens with uniform confidence. It may be beneficial to deprioritize fitting tokens that serve grammatical functions rather than carrying primary semantic content. This concept is analogous to human pedagogy, where students are taught to focus on substantive concepts rather than perfecting the usage of common connective words. Further analysis can be found in Appendix A.4.

5 CONCLUSION

In this work, we address the well-documented generalization gap between Supervised Fine-Tuning and Reinforcement Learning. We provide a novel theoretical analysis, demonstrating that the standard SFT gradient is equivalent to a policy gradient update with an ill-posed implicit reward that is inversely proportional to the model’s confidence. This insight explains SFT’s tendency to overfit and its unstable optimization dynamics. Building on this analysis, we introduce DFT, a simple yet powerful method that rectifies this issue by dynamically reweighting the SFT loss with the token probability. This one-line modification stabilizes the learning process and promotes better generalization. Our extensive experiments show that DFT consistently outperforms standard SFT across

various models and challenging mathematical reasoning benchmarks. Furthermore, when adapted to an offline RL setting, DFT surpasses established online and offline RL algorithms, highlighting its effectiveness and efficiency. Our work provides both a deeper understanding of SFT and a practical, high-impact solution that significantly closes the performance gap with more complex RL methods.

REFERENCES

- Abbas Abdolmaleki, Bilal Piot, Bobak Shahriari, Jost Tobias Springenberg, Tim Hertweck, Michael Bloesch, Rishabh Joshi, Thomas Lampe, Junhyuk Oh, Nicolas Heess, et al. Learning from negative feedback, or positive feedback or both. In *ICLR*, 2025. [3](#)
- Janice Ahn, Rishu Verma, Renze Lou, Di Liu, Rui Zhang, and Wenpeng Yin. Large language models for mathematical reasoning: Progresses and challenges. In *EACLW*, pp. 225–237, 2024. [2](#), [6](#), [7](#)
- American Institute of Mathematics. Aime 2024 competition mathematical problems, 2024. [2](#), [5](#)
- Yuntao Bai, Andy Jones, Kamal Ndousse, Amanda Askell, Anna Chen, Nova Dasgupta, Dawn Drain, Stanislav Fort, Deep Ganguli, Tom Hase, et al. Training a helpful and harmless assistant with reinforcement learning from human feedback. *arXiv preprint arXiv:2204.05862*, 2022. [1](#), [2](#)
- Federico Cassano, John Gouwar, Daniel Nguyen, Sydney Nguyen, Luna Phipps-Costin, Donald Pinckney, Ming-Ho Yee, Yangtian Zi, Carolyn Jane Anderson, Molly Q Feldman, et al. Multipl-e: A scalable and polyglot approach to benchmarking neural code generation. *IEEE Transactions on Software Engineering*, 49(7):3675–3691, 2023. [8](#)
- Huayu Chen, Kaiwen Zheng, Qinsheng Zhang, Ganqu Cui, Yin Cui, Haotian Ye, Tsung-Yi Lin, Ming-Yu Liu, Jun Zhu, and Haoxiang Wang. Bridging supervised learning and reinforcement learning in math reasoning. *arXiv preprint arXiv:2505.18116*, 2025a. [2](#)
- Mark Chen, Jerry Tworek, Heewoo Jun, Qiming Yuan, Henrique Ponde De Oliveira Pinto, Jared Kaplan, Harri Edwards, Yuri Burda, Nicholas Joseph, Greg Brockman, et al. Evaluating large language models trained on code. *arXiv preprint arXiv:2107.03374*, 2021. [7](#)
- Zhipeng Chen, Yingqian Min, Beichen Zhang, Jie Chen, Jinhao Jiang, Daixuan Cheng, Wayne Xin Zhao, Zheng Liu, Xu Miao, Yang Lu, Lei Fang, Zhongyuan Wang, and Ji-Rong Wen. An empirical study on eliciting and improving r1-like reasoning models. *arXiv preprint arXiv:2503.04548*, 2025b. [1](#)
- Paul F Christiano, Jan Leike, Tom Brown, Miljan Martic, Shane Legg, and Dario Amodei. Deep reinforcement learning from human preferences. In *NeurIPS*, volume 30, 2017. [1](#), [2](#)
- Tianzhe Chu, Yuexiang Zhai, Jihan Yang, Shengbang Tong, Saining Xie, Dale Schuurmans, Quoc V Le, Sergey Levine, and Yi Ma. Sft memorizes, rl generalizes: A comparative study of foundation model post-training. In *ICML*, 2024. [1](#), [2](#)
- Hyung Won Chung, Le Hou, Shayne Longpre, Barret Zoph, Yi Tay, William Fedus, Yunxuan Li, Xuezhi Wang, Mostafa Dehghani, Siddhartha Brahma, et al. Scaling instruction-finetuned language models. *Journal of Machine Learning Research*, 25(70):1–53, 2024. [1](#), [2](#)
- Ganqu Cui, Lifan Yuan, Ning Ding, Guanming Yao, Bingxiang He, Wei Zhu, Yuan Ni, Guotong Xie, Ruobing Xie, Yankai Lin, et al. Ultrafeedback: boosting language models with scaled ai feedback. In *ICML*, pp. 9722–9744, 2024. [7](#)
- DeepSeek-AI, Daya Guo, Dejian Yang, Haowei Zhang, Junxiao Song, Ruoyu Zhang, Runxin Xu, Qihao Zhu, Shirong Ma, Peiyi Wang, Xiao Bi, Xiaokang Zhang, Xingkai Yu, Yu Wu, Z. F. Wu, Zhibin Gou, Zhihong Shao, Zhuoshu Li, Ziyi Gao, Aixin Liu, Bing Xue, Bingxuan Wang, Bochao Wu, Bei Feng, Chengda Lu, Chenggang Zhao, Chengqi Deng, Chenyu Zhang, Chong Ruan, Damai Dai, Deli Chen, Dongjie Ji, Erhang Li, Fangyun Lin, Fucong Dai, Fuli Luo, Guangbo Hao, Guanting Chen, Guowei Li, H. Zhang, Han Bao, Hanwei Xu, Haocheng Wang, Honghui Ding, Huajian Xin, Huazuo Gao, Hui Qu, Hui Li, Jianzhong Guo, Jiashi Li, Jiawei Wang, Jingchang Chen, Jingyang Yuan, Junjie Qiu, Junlong Li, J. L. Cai, Jiaqi Ni, Jian Liang, Jin Chen, Kai Dong, Kai Hu, Kaige Gao, Kang Guan, Kexin Huang, Kuai Yu, Lean Wang, Lecong Zhang,

Liang Zhao, Litong Wang, Liyue Zhang, Lei Xu, Leyi Xia, Mingchuan Zhang, Minghua Zhang, Minghui Tang, Meng Li, Miaojun Wang, Mingming Li, Ning Tian, Panpan Huang, Peng Zhang, Qiancheng Wang, Qinyu Chen, Qiushi Du, Ruiqi Ge, Ruisong Zhang, Ruizhe Pan, Runji Wang, R. J. Chen, R. L. Jin, Ruyi Chen, Shanghao Lu, Shangyan Zhou, Shanhua Chen, Shengfeng Ye, Shiyu Wang, Shuiping Yu, Shunfeng Zhou, Shuting Pan, S. S. Li, Shuang Zhou, Shaoqing Wu, Shengfeng Ye, Tao Yun, Tian Pei, Tianyu Sun, T. Wang, Wangding Zeng, Wanjia Zhao, Wen Liu, Wenfeng Liang, Wenjun Gao, Wenqin Yu, Wentao Zhang, W. L. Xiao, Wei An, Xiaodong Liu, Xiaohan Wang, Xiaokang Chen, Xiaotao Nie, Xin Cheng, Xin Liu, Xin Xie, Xingchao Liu, Xinyu Yang, Xinyuan Li, Xuecheng Su, Xuheng Lin, X. Q. Li, Xiangyue Jin, Xiaojin Shen, Xiaosha Chen, Xiaowen Sun, Xiaoxiang Wang, Xinnan Song, Xinyi Zhou, Xianzu Wang, Xinxia Shan, Y. K. Li, Y. Q. Wang, Y. X. Wei, Yang Zhang, Yanhong Xu, Yao Li, Yao Zhao, Yaofeng Sun, Yaohui Wang, Yi Yu, Yichao Zhang, Yifan Shi, Yiliang Xiong, Ying He, Yishi Piao, Yisong Wang, Yixuan Tan, Yiyang Ma, Yiyuan Liu, Yongqiang Guo, Yuan Ou, Yuduan Wang, Yue Gong, Yuheng Zou, Yujia He, Yunfan Xiong, Yuxiang Luo, Yuxiang You, Yuxuan Liu, Yuyang Zhou, Y. X. Zhu, Yanhong Xu, Yanping Huang, Yaohui Li, Yi Zheng, Yuchen Zhu, Yunxian Ma, Ying Tang, Yukun Zha, Yuting Yan, Z. Z. Ren, Zehui Ren, Zhangli Sha, Zhe Fu, Zhean Xu, Zhenda Xie, Zhengyan Zhang, Zhewen Hao, Zhicheng Ma, Zhigang Yan, Zhiyu Wu, Zihui Gu, Zijia Zhu, Zijun Liu, Zilin Li, Ziwei Xie, Ziyang Song, Zizheng Pan, Zhen Huang, Zhipeng Xu, Zhongyu Zhang, and Zhen Zhang. Deepseek-r1: Incentivizing reasoning capability in llms via reinforcement learning, 2025. [4](#), [16](#)

Hanze Dong, Wei Xiong, Deepanshu Goyal, Yihan Zhang, Winnie Chow, Rui Pan, Shizhe Diao, Jipeng Zhang, Kashun Shum, and Tong Zhang. Raft: Reward ranked finetuning for generative foundation model alignment. *Transactions on Machine Learning Research*, 2023, 2023. [2](#), [6](#), [7](#)

Yilun Du et al. Simplify rlhf as reward-weighted sft: A variational method. *arXiv preprint arXiv:2502.11026*, 2025. [3](#), [7](#)

Haodong Duan, Junming Yang, Yuxuan Qiao, Xinyu Fang, Lin Chen, Yuan Liu, Xiaoyi Dong, Yuhang Zang, Pan Zhang, Jiaqi Wang, et al. Vlmevalkit: An open-source toolkit for evaluating large multi-modality models. In *ACM MM*, pp. 11198–11201, 2024. [8](#)

Abhimanyu Dubey, Abhinav Jauhri, Abhinav Pandey, Abhishek Kadian, Ahmad Al-Dahle, Aiesha Letman, Akhil Mathur, Alan Schelten, Amy Yang, Angela Fan, et al. The llama 3 herd of models. *arXiv preprint arXiv:2407.21783*, 2024. [5](#)

Yoav Freund. A more robust boosting algorithm. *arXiv preprint arXiv:0905.2138*, 2009. [15](#)

Chaoqun He, Renjie Luo, Yuzhuo Bai, Shengding Hu, Zhen Thai, Junhao Shen, Jinyi Hu, Xu Han, Yujie Huang, Yuxiang Zhang, et al. Olympiadbench: A challenging benchmark for promoting agi with olympiad-level bilingual multimodal scientific problems. In *ACL*, pp. 3828–3850, 2024. [2](#), [5](#)

Dan Hendrycks, Collin Burns, Saurav Kadavath, Akul Arora, Steven Basart, Eric Tang, Dawn Song, and Jacob Steinhardt. Measuring mathematical problem solving with the math dataset. In *NeurIPS*, 2021. [5](#)

Edward J Hu, Yelong Shen, Phillip Wallis, Zeyuan Allen-Zhu, Yuanzhi Li, Shean Wang, Lu Wang, Weizhu Chen, et al. Lora: Low-rank adaptation of large language models. *ICLR*, 1(2):3, 2022. [6](#)

Maggie Huan, Yuetai Li, Tuney Zheng, Xiaoyu Xu, Seungone Kim, Minxin Du, Radha Poovendran, Graham Neubig, and Xiang Yue. Does math reasoning improve general llm capabilities? understanding transferability of llm reasoning. *arXiv preprint arXiv:2507.00432*, 2025. [1](#)

Hugging Face. Open r1: A fully open reproduction of deepseek-r1, January 2025. [6](#), [16](#)

Sergey Levine, Aviral Kumar, George Tucker, and Justin Fu. Offline reinforcement learning: Tutorial, review, and perspectives on open problems. *arXiv preprint arXiv:2005.01643*, 2020. [2](#)

Aitor Lewkowycz, Anders Andreassen, David Dohan, Ethan Dyer, Henryk Michalewski, Vinay Ramasesh, Ambrose Slone, Cem Anil, Imanol Schlag, Theo Gutman-Solo, et al. Solving quantitative reasoning problems with language models. *NeurIPS*, 35:3843–3857, 2022. [5](#)

- Jia LI, Edward Beeching, Lewis Tunstall, Ben Lipkin, Roman Soletskyi, Shengyi Costa Huang, Kashif Rasul, Longhui Yu, Albert Jiang, Ziju Shen, Zihan Qin, Bin Dong, Li Zhou, Yann Fleureau, Guillaume Lample, and Stanislas Polu. Numinamath, 2024. [2](#), [5](#)
- Tsung-Yi Lin, Priya Goyal, Ross Girshick, Kaiming He, and Piotr Dollár. Focal loss for dense object detection. In *ICCV*, pp. 2999–3007, 2017. [3](#)
- Jiawei Liu, Chunqiu Steven Xia, Yuyao Wang, and Lingming Zhang. Is your code generated by chatgpt really correct? rigorous evaluation of large language models for code generation. *NeurIPS*, 36:21558–21572, 2023. [7](#)
- Mingyang Liu, Gabriele Farina, and Asuman Ozdaglar. Uft: Unifying supervised and reinforcement fine-tuning. *arXiv preprint arXiv:2505.16984*, 2025. [1](#), [2](#)
- Vivian Liu and Yiqiao Yin. Green ai: exploring carbon footprints, mitigation strategies, and trade offs in large language model training. *Discover Artificial Intelligence*, 4(49), 2024. [1](#)
- Ajay Mandlekar, Danfei Xu, Josiah Wong, Soroush Nasiriany, Chen Wang, Rohun Kulkarni, Li Fei-Fei, Silvio Savarese, Yuke Zhu, and Roberto Martín-Martín. What matters in learning from offline human demonstrations for robot manipulation. In *CoRL*, pp. 1678–1690, 2022. [1](#), [2](#)
- Mathematical Association of America. Amc 2023 competition problems, 2023. [2](#), [5](#)
- Long Ouyang, Jeffrey Wu, Xu Jiang, Diogo Almeida, Carroll Wainwright, Pamela Mishkin, Chong Zhang, Sandhini Agarwal, Katarina Slama, Alex Ray, et al. Training language models to follow instructions with human feedback. *NeurIPS*, 35:27730–27744, 2022. [1](#), [2](#)
- Richard Yuanzhe Pang and He He. Text generation by learning from demonstrations. In *ICLR*, 2021. [3](#)
- Runqi Qiao, Qiuna Tan, Guanting Dong, Minhui Wu, Chong Sun, Xiaoshuai Song, Zhuoma GongQue, Shanglin Lei, Zhe Wei, MiaoXuan Zhang, et al. We-math: Does your large multimodal model achieve human-like mathematical reasoning? *arXiv preprint arXiv:2407.01284*, 2024. [8](#)
- Chongli Qin and Jost Tobias Springenberg. Supervised fine tuning on curated data is reinforcement learning (and can be improved). *arXiv preprint arXiv:2507.12856*, 2025. [3](#), [6](#), [15](#)
- Haibo Qiu, Xiaohan Lan, Fanfan Liu, Xiaohu Sun, Delian Ruan, Peng Shi, and Lin Ma. Metis-rise: RL incentivizes and sft enhances multimodal reasoning model learning. *arXiv preprint arXiv:2506.13056*, 2025. [1](#), [2](#)
- Qwen Team, An Yang, Baosong Yang, Beichen Zhang, Binyuan Hui, Bo Zheng, Bowen Yu, Chengyuan Li, Dayiheng Liu, Fei Huang, et al. Qwen2.5: A party of foundation models. *arXiv preprint arXiv:2412.15115*, 2024a. [5](#)
- Qwen Team, An Yang, Baosong Yang, Beichen Zhang, Binyuan Hui, Bo Zheng, Bowen Yu, Chengyuan Li, Dayiheng Liu, Fei Huang, et al. Qwen2.5 technical report. *arXiv preprint arXiv:2412.15115*, 2024b. [2](#)
- Rafael Rafailov, Archit Sharma, Eric Mitchell, Christopher D Manning, Stefano Ermon, and Chelsea Finn. Direct preference optimization: Your language model is secretly a reward model. In *NeurIPS*, volume 36, 2023. [1](#), [2](#), [7](#)
- Claude Sammut. *Behavioral Cloning*. 2011. [2](#)
- Victor Sanh, Albert Webson, Colin Raffel, Stephen Bach, Lintang Sutton, Zaid Alyafeai, Antoine Chaffin, Arnaud Stiegler, Teven Le Scao, Arun Raja, et al. Multitask prompted training enables zero-shot task generalization. In *ICLR*, 2022. [1](#)
- Fumihiro Sasaki and Ryota Yamashina. Behavioral cloning from noisy demonstrations. In *ICLR*, 2020. [15](#)
- John Schulman, Filip Wolski, Prafulla Dhariwal, Alec Radford, and Oleg Klimov. Proximal policy optimization algorithms. *arXiv preprint arXiv:1707.06347*, 2017. [1](#), [2](#), [4](#), [7](#)

- Zhihong Shao, Peiyi Wang, Qihao Zhu, Runxin Xu, Junxiao Song, Xiao Bi, Haowei Zhang, Mingchuan Zhang, YK Li, Yang Wu, et al. Deepseekmath: Pushing the limits of mathematical reasoning in open language models. *arXiv preprint arXiv:2402.03300*, 2024. [5](#), [7](#)
- Guangming Sheng, Chi Zhang, Zilingfeng Ye, Xibin Wu, Wang Zhang, Ru Zhang, Yanghua Peng, Haibin Lin, and Chuan Wu. Hybridflow: A flexible and efficient rlhf framework. In *ECCV*, pp. 1279–1297, 2025. [1](#), [2](#), [5](#), [7](#)
- Emma Strubell, Ananya Ganesh, and Andrew McCallum. Energy and policy considerations for deep learning in nlp. In *ACL*, pp. 3645–3650, 2019. [1](#), [2](#)
- Gokul Swamy, Sanjiban Choudhury, Wen Sun, Zhiwei Steven Wu, and J Andrew Bagnell. All roads lead to likelihood: The value of reinforcement learning in fine-tuning. *arXiv preprint arXiv:2503.01067*, 2025. [1](#), [2](#)
- Bo Wang, Qinyuan Cheng, Runyu Peng, Rong Bao, Peiji Li, Qipeng Guo, Linyang Li, Zhiyuan Zeng, Yunhua Zhou, and Xipeng Qiu. Implicit reward as the bridge: A unified view of sft and dpo connections. *arXiv preprint arXiv:2507.00018*, 2025. [3](#)
- Ke Wang, Junting Pan, Weikang Shi, Zimu Lu, Houxing Ren, Aojun Zhou, Mingjie Zhan, and Hongsheng Li. Measuring multimodal mathematical reasoning with math-vision dataset. In *NeurIPS*, 2024. [8](#)
- Jason Wei, Maarten Bosma, Vincent Zhao, Kelvin Guu, Adams Wei Yu, Brian Lester, Nan Du, Andrew M Dai, and Quoc V Le. Finetuned language models are zero-shot learners. In *ICLR*, 2022. [1](#), [2](#)
- Jenis Winsta. The hidden costs of ai: A review of energy, e-waste, and inequality in model development. *arXiv preprint arXiv:2507.09611*, 2025. [1](#)
- Jianhao Yan, Yafu Li, Zican Hu, Zhi Wang, Ganqu Cui, Xiaoye Qu, Yu Cheng, and Yue Zhang. Learning to reason under off-policy guidance. *arXiv preprint arXiv:2504.14945*, 2025. [16](#)
- Jie Yang, Feipeng Ma, Zitian Wang, Dacheng Yin, Kang Rong, Fengyun Rao, and Ruimao Zhang. Wethink: Toward general-purpose vision-language reasoning via reinforcement learning. *arXiv preprint arXiv:2506.07905*, 2025. [8](#)
- Qingyang Zhang, Haitao Wu, Changqing Zhang, Peilin Zhao, and Yatao Bian. Right question is already half the answer: Fully unsupervised llm reasoning incentivization. *arXiv preprint arXiv:2504.05812*, 2025. [2](#)
- Renrui Zhang, Dongzhi Jiang, Yichi Zhang, Haokun Lin, Ziyu Guo, Pengshuo Qiu, Aojun Zhou, Pan Lu, Kai-Wei Chang, Yu Qiao, et al. Mathverse: Does your multi-modal llm truly see the diagrams in visual math problems? In *ECCV*, pp. 169–186, 2024a. [8](#)
- Shengyu Zhang, Linfeng Dong, Xiaoya Li, Sen Zhang, Xiaofei Sun, Shuhe Wang, Jiwei Li, Runyi Hu, Tianwei Zhang, Fei Wu, and Guoyin Wang. Instruction tuning for large language models: A survey. *arXiv preprint arXiv:2308.10792*, 2024b. [1](#)
- Shiyue Zhang, Shijie Wu, Ozan Irsoy, Steven Lu, Mohit Bansal, Mark Dredze, and David Rosenberg. Mixce: Training autoregressive language models by mixing forward and reverse cross-entropies. In *ACL*, pp. 9027–9050, 2023. [3](#)
- Yuze Zhao, Jintao Huang, Jingjun Hu, Xingjun Wang, Yunlin Mao, Daoze Zhang, Zeyinzi Jiang, Zhikai Wu, Baole Ai, Ang Wang, Wenmeng Zhou, and Yingda Chen. Swift:a scalable lightweight infrastructure for fine-tuning, 2024. [7](#)
- Yaowei Zheng, Richong Zhang, Junhao Zhang, YeYanhan YeYanhan, and Zheyuan Luo. Llamafactory: Unified efficient fine-tuning of 100+ language models. In *ACL*, pp. 400–410, 2024. [8](#)
- Chunting Zhou, Pengfei Liu, Puxin Xu, Srinivasan Iyer, Jianfeng Sun, Yuning Mao, Xuezhe Ma, Avia Efrat, Ping Yu, Lili Yu, et al. Lima: Less is more for alignment. In *NeurIPS*, volume 36, 2023. [1](#), [2](#)

A APPENDIX

A.1 USAGE OF LLM

We employ LLM primarily as writing assistants to refine and polish the manuscript. Their usage was limited to improving clarity, coherence, and presentation, while all conceptual and experimental contributions remain original.

A.2 LIMITATIONS

While our experiments demonstrate the effectiveness of DFT on mathematical reasoning benchmarks and code generation tasks, the evaluation scope remains limited. We have not yet assessed its performance on broader task categories or with larger-scale LLM, which we leave for future exploration. Moreover, DFT may not offer universal benefits across all scenarios. In domains that primarily involve the acquisition of factual knowledge, conventional SFT may remain the most efficient approach. Our aim is not to assert that DFT universally outperforms SFT, but rather to offer a new perspective on objective design by analyzing the distinction between RL and SFT.

A.3 DETAILED DERIVATION OF EQUATION (5)

We start from the SFT gradient in Equation (2):

$$\nabla_{\theta} \mathcal{L}_{\text{SFT}}(\theta) = \mathbb{E}_{(x, y^*) \sim \mathcal{D}} [-\nabla_{\theta} \log \pi_{\theta}(y^* | x)]. \quad (1)$$

For each query x , the expectation over expert demonstrations (x, y^*) can be written explicitly as a summation over all possible outputs y :

$$\mathbb{E}_{(x, y^*) \sim \mathcal{D}} [-\nabla_{\theta} \log \pi_{\theta}(y^* | x)] = \mathbb{E}_{x \sim \mathcal{D}_x} \sum_y \mathbf{1}[y = y^*] [-\nabla_{\theta} \log \pi_{\theta}(y | x)]. \quad (2)$$

We insert the model distribution $\pi_{\theta}(y | x)$, which allows us to express the summation in terms of importance weights:

$$\mathbb{E}_{x \sim \mathcal{D}_x} \sum_y \pi_{\theta}(y | x) \cdot \frac{\mathbf{1}[y = y^*]}{\pi_{\theta}(y | x)} [-\nabla_{\theta} \log \pi_{\theta}(y | x)]. \quad (3)$$

Here, the term $\frac{\mathbf{1}[y = y^*]}{\pi_{\theta}(y | x)}$ serves as an importance weight comparing the expert (Dirac delta) distribution with the model's distribution.

The summation over y can now be rewritten as an expectation under the policy distribution $y \sim \pi_{\theta}(\cdot | x)$:

$$\mathbb{E}_{x \sim \mathcal{D}_x} \mathbb{E}_{y \sim \pi_{\theta}(\cdot | x)} \left[\frac{\mathbf{1}[y = y^*]}{\pi_{\theta}(y | x)} (-\nabla_{\theta} \log \pi_{\theta}(y | x)) \right]. \quad (4)$$

Thus, we obtain Equation (5):

$$\mathbb{E}_{(x, y^*) \sim \mathcal{D}} [-\nabla_{\theta} \log \pi_{\theta}(y^* | x)] = \mathbb{E}_{x \sim \mathcal{D}_x} \mathbb{E}_{y \sim \pi_{\theta}(\cdot | x)} \left[\frac{\mathbf{1}[y = y^*]}{\pi_{\theta}(y | x)} (-\nabla_{\theta} \log \pi_{\theta}(y | x)) \right]. \quad (5)$$

This derivation shows that the SFT gradient can be expressed as an on-policy policy gradient with importance sampling, where the expert demonstration distribution is reweighted relative to the model distribution.

A.4 DISCUSSIONS AND INSIGHTS

Gradient Analysis of DFT. We now analyze the gradient induced by the DFT surrogate loss. Recall the sequence-level definition:

$$\mathcal{L}_{\text{DFT}}(\theta) = -\text{sg}(\pi_{\theta}(y^* | x)) \log \pi_{\theta}(y^* | x), \quad (10)$$

where $\text{sg}(\cdot)$ denotes the stop-gradient operator. Since the stop-gradient blocks backpropagation, the detached probability $\text{sg}(\pi_\theta(y^* | x))$ is treated as a constant during differentiation. Consequently, the gradient becomes

$$\nabla_\theta \mathcal{L}_{\text{DFT}} = -\text{sg}(\pi_\theta(y^* | x)) \frac{1}{\pi_\theta(y^* | x)} \nabla_\theta \pi_\theta(y^* | x) \quad (11)$$

$$= -\left(\frac{\text{sg}(\pi_\theta(y^* | x))}{\pi_\theta(y^* | x)}\right) \nabla_\theta \pi_\theta(y^* | x). \quad (12)$$

Since $\text{sg}(\pi_\theta(y^* | x))$ equals $\pi_\theta(y^* | x)$ in the forward pass, the prefactor is numerically equal to 1. Therefore,

$$\nabla_\theta \mathcal{L}_{\text{DFT}} = -\nabla_\theta \pi_\theta(y^* | x). \quad (13)$$

This shows that DFT is mathematically equivalent to directly maximizing the model probability of the target token, rather than its log-probability as in cross-entropy.

For cross-entropy, the loss is

$$\mathcal{L}_{\text{CE}}(\theta) = -\log \pi_\theta(y^* | x),$$

yielding gradient

$$\nabla_\theta \mathcal{L}_{\text{CE}} = -\frac{1}{\pi_\theta(y^* | x)} \nabla_\theta \pi_\theta(y^* | x).$$

Thus both CE and DFT share the same gradient direction but differ in scaling: CE amplifies updates for low-probability targets (factor $1/\pi$), while DFT applies a uniform factor 1. As a result, DFT avoids the instability caused by excessively large gradients on unlikely expert tokens, providing more conservative and stable updates.

From the reinforcement learning perspective, the reward of DFT becomes uniformly 1 across all expert trajectories, equivalent to a verification-style objective that treats all correct references equally. From the optimization perspective, DFT trades off aggressive fitting of rare tokens for better stability and calibration. Practically, this explains why DFT often yields smoother training and stronger generalization, while maintaining alignment with the pre-training distribution.

Learning from Noisy Data. DFT offers a simple yet effective approach, prompting us to reflect on why it might actually work. One intuitive explanation lies in its ability to learn from noisy data (Freund, 2009). Sasaki & Yamashina (2020) propose an imitation learning algorithm for learning from noisy demonstrations, based on the core idea of avoiding the fitting of data that is difficult to model, as such data is likely to originate from suboptimal behaviors, i.e., noise. Their method introduces a weighted behavioral cloning objective, where the weights are derived from a previously trained policy’s confidence in each action. Similarly, the weighting mechanism in DFT shares the same intuition, but instead of relying on a fixed old policy model to compute confidence scores, it uses a single policy model to perform confidence-based weighting on-the-fly during training.

A.5 COMPARISON WITH CONCURRENT WORK IW-SFT

We include a concurrent method, Importance-Weighted SFT (iw-SFT) (Qin & Springenberg, 2025), for comparison. All training settings follow those reported in the original paper, except that we set the number of training epochs to 1.

As shown in Table 5, DFT achieves higher average accuracy than iw-SFT on most model families: LLaMA-3.2-3B (+2.39), LLaMA-3.1-8B (+4.15), DeepSeekMath-7B (+3.34), and Qwen2.5-Math-1.5B (+1.30). Although iw-SFT outperforms our method on Qwen2.5-Math-7B (+2.45), this improvement is not consistent across datasets. In particular, for LLaMA-3.2-3B, iw-SFT underperforms standard SFT on Math500 (5.13 vs. 8.65) and AMC23 (2.03 vs. 3.13). Similarly, for LLaMA-3.1-8B, iw-SFT results in worse performance than SFT on Minerva Math (4.31 vs. 5.78) and AMC23 (7.34 vs. 8.28). In contrast, DFT consistently improves upon both the base model and SFT across nearly all datasets, including those where iw-SFT fails. These results underline better generalization ability of DFT in diverse mathematical reasoning scenarios. Moreover, iw-SFT incurs additional computational overhead by requiring a separate reference model to compute importance weights, whereas DFT dynamically derives its own weighting directly from the token probabilities of model, resulting in a more efficient training procedure.

Table 5: Comparison with concurrent work iw-SFT on math benchmarks. DFT outperforms the iw-SFT in most settings across model families and benchmarks. The best performance is bold.

	Math500	Minerva Math	Olympiad Bench	AIME24	AMC23	Avg.
LLaMA-3.2-3B w/iw-SFT	5.13	2.63	1.51	0.00	2.03	2.26
LLaMA-3.2-3B w/DFT	12.79	2.84	2.90	0.83	3.91	4.65
LLaMA-3.1-8B w/iw-SFT	18.21	4.31	4.31	0.20	7.34	6.87
LLaMA-3.1-8B w/DFT	27.44	8.26	6.94	0.41	12.03	11.02
DeepSeekMath-7B w/iw-SFT	35.32	8.75	11.11	0.61	18.28	14.81
DeepSeekMath-7B w/DFT	41.46	16.79	15.00	1.24	16.25	18.15
Qwen2.5-Math-1.5B w/iw-SFT	59.38	17.08	26.82	8.13	40.00	30.28
Qwen2.5-Math-1.5B w/DFT	64.89	20.94	27.08	6.87	38.13	31.58
Qwen2.5-Math-7B w/iw-SFT	70.28	25.70	34.46	16.46	51.09	39.60
Qwen2.5-Math-7B w/DFT	68.20	30.16	33.83	8.56	45.00	37.15

Table 6: Evaluation results on five mathematical reasoning benchmarks in the offline reinforcement learning setting using rejection-sampling-based reward signals, compared against iw-SFT.

	Setting	Math500	Minerva Math	Olympiad Bench	AIME24	AMC23	Avg.
Qwen2.5-Math-1.5B w/iw-SFT	SFT	59.38	17.08	26.82	8.13	40.00	30.28
Qwen2.5-Math-1.5B w/DFT	SFT	62.50	22.94	26.87	7.31	33.75	30.67
Qwen2.5-Math-1.5B w/iw-SFT	Offline	60.80	18.13	27.83	8.33	44.21	31.86
Qwen2.5-Math-1.5B w/DFT	Offline	64.71	25.16	30.93	7.93	48.44	35.43

We also compare against iw-SFT under the offline setting, as shown in Table 6. While iw-SFT performs competitively on certain datasets, achieving 60.80 on Math500 and 44.21 on AMC23, its overall average performance (31.86) remains below that of our method by +3.57 points. Moreover, iw-SFT shows only modest improvements compared to its standard SFT counterpart, with an average score of 31.86 in the offline RL setting versus 30.28 with SFT (+1.58). In contrast, DFT achieves a larger gain of +4.76 (from 30.67 to 35.43). These results indicate that iw-SFT provides limited benefits from reward supervision under offline constraints, whereas DFT is able to more effectively incorporate such signals, leading to better generalization and higher task performance.

A.6 EXPLORATORY EXPERIMENT - OPENR1-MATH TRAINING DATASET

Inspired by DeepSeek-R1 [DeepSeek-AI et al. \(2025\)](#), several studies have attempted to train open-source models to reproduce its reasoning capabilities ([Hugging Face, 2025](#)). To this end, a high-quality dataset, OpenR1-Math-220k ([Hugging Face, 2025](#)), was constructed, where the prompts are drawn from NuminaMath 1.5 and the off-policy reasoning traces are generated by DeepSeek-R1. LUFFY ([Yan et al., 2025](#)) further filtered out sequences longer than 8192 tokens as well as those verified incorrect by Math-Verify, resulting in about 45k prompts paired with off-policy reasoning traces. We adopt this dataset as the training corpus for SFT. All training details remain the same as previous experiments, except that the number of epochs is set to 3.

As shown in Table 7, training on OpenR1-Math-220k consistently improves performance, and the use of higher-quality annotations yields additional gains. SFT on this dataset increases the average accuracy of Qwen2.5-Math-1.5B by +13.24 points compared to the base model, while DFT provides a further +9.03 gain, resulting in a total improvement of +22.27. These results suggest that DFT remains effective even when applied on top of high-quality training data, highlighting its potential as a general fine-tuning paradigm.

Table 7: Performance training on the OpenR1-Math-220k dataset. The best score for each benchmark is in bold.

	Math500	Minerva Math	Olympiad Bench	AIME24	AMC23	Avg.
Qwen2.5-Math-1.5B	31.66	8.51	15.88	4.16	19.38	15.92
Qwen2.5-Math-1.5B w/SFT	61.60	20.29	24.27	4.16	35.47	29.16
Qwen2.5-Math-1.5B w/DFT	71.76	27.00	33.48	9.79	48.91	38.19

Table 8: Performance on five mathematical reasoning benchmarks using LoRA for training. The best score of each model across benchmarks is highlighted in bold.

	Math500	Minerva Math	Olympiad Bench	AIME24	AMC23	Avg.
LLaMA-3.2-3B	1.63	1.36	1.01	0.41	1.56	1.19
LLaMA-3.2-3B w/SFT	4.88	1.56	1.68	0.00	2.66	2.56
LLaMA-3.2-3B w/DFT	11.13	5.18	3.87	0.00	2.97	4.63
Qwen2.5-Math-1.5B	31.66	8.51	15.88	4.16	19.38	15.92
Qwen2.5-Math-1.5B w/SFT	41.47	10.85	11.56	1.45	17.03	16.87
Qwen2.5-Math-1.5B w/DFT	64.85	22.58	28.45	5.84	40.78	32.90

A.7 EXPLORATORY EXPERIMENT - PEFT TRAINING SETTING

To investigate whether DFT remains effective under parameter-efficient fine-tuning (PEFT) settings with limited compute, we apply DFT using LoRA adapters across two model families: LLaMA-3.2-3B and Qwen2.5-Math-1.5B. All training configurations remain identical to previous full-parameter experiments, except that LoRA is enabled with rank=8 and alpha=16.

As shown in Table 8, DFT provides consistent improvements over both base and SFT baselines under LoRA-based PEFT. For Qwen2.5-Math-1.5B, DFT increases the average accuracy from 15.92 (base) and 16.87 (SFT) to 32.90. For LLaMA-3.2-3B, DFT achieves a gain of +3.44 over SFT (from 1.19 to 4.63). These results indicate that DFT can serve as an effective fine-tuning strategy in low-resource or compute-constrained settings, where full model updates are not practical.

A.8 TRAINING HYPER-PARAMETERS ABLATION

To assess the robustness and sensitivity of our approach (DFT) with respect to key training hyperparameters, we conduct an ablation study focused on learning rate and batch size, using the Qwen2.5-Math-1.5B base model. This analysis aims to answer two central questions: (1) Is the performance gap between DFT and SFT due to a suboptimal hyperparameter configuration in SFT? (2) How sensitive are both methods to changes in learning rate and batch size?

We evaluate both DFT and SFT across four learning rates: 2e-4, 1e-4, 5e-5, and 1e-5. As shown in Figure 3 (left), both methods exhibit a certain degree of sensitivity to the learning rate. DFT consistently outperforms SFT under all configurations, suggesting that the performance gap cannot be attributed solely to suboptimal hyperparameter choices in SFT. For both methods, intermediate learning rates (1e-4 and 5e-5) yield the best results, while both lower (1e-5) and higher (2e-4) values lead to noticeable degradation.

We further assess the impact of batch size, sweeping values from 32 to 256. As shown in Figure 3 (right), both DFT and SFT exhibit relatively stable performance across the full range of batch sizes. While minor fluctuations are observed, there is no consistent trend indicating that larger or smaller batches significantly affect final accuracy. This suggests that batch size is not a dominant factor for either method in this setup, and that default values may suffice in practice.

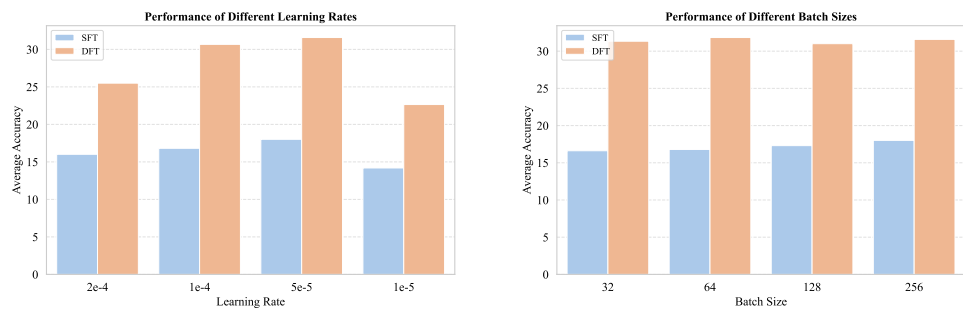


Figure 3: Ablation study of training hyper-parameters, learning rates and batch size, for DFT and SFT on Qwen2.5-Math-1.5B model.